Phase Diagram of Patchy Colloids: Towards Empty Liquids

Emanuela Bianchi,[1] Julio Largo,[2] Piero Tartaglia,[1] Emanuela Zaccarelli,[3] and Francesco Sciortino[3]

[1]*Dipartimento di Fisica and CNR-INFM-SMC, Università di Roma La Sapienza, Piazzale A. Moro 2, 00185 Roma, Italy*
[2]*Dipartimento di Fisica, Università di Roma La Sapienza, Piazzale A. Moro 2, 00185 Roma, Italy*
[3]*Dipartimento di Fisica and CNR-INFM-SOFT, Università di Roma La Sapienza, Piazzale A. Moro 2, 00185 Roma, Italy*

(Received 30 May 2006; published 16 October 2006)

We report theoretical and numerical evaluations of the phase diagram for patchy colloidal particles of new generation. We show that the reduction of the number of bonded nearest neighbors offers the possibility of generating liquid states (i.e., states with temperature T lower than the liquid-gas critical temperature) with a vanishing occupied packing fraction (ϕ), a case which can not be realized with spherically interacting particles. Theoretical results suggest that such reduction is accompanied by an increase of the region of stability of the liquid phase in the (T-ϕ) plane, possibly favoring the establishment of homogeneous disordered materials at small ϕ, i.e., stable equilibrium gels.

DOI: 10.1103/PhysRevLett.97.168301 PACS numbers: 82.70.Dd, 61.20.Ja, 82.70.Gg

The physico-chemical manipulation of colloidal particles is growing at an incredible pace. The large freedom in the control of the interparticle potential has made it possible to design colloidal particles which significantly extend the possibilities offered by atomic systems [1]. An impressive step further is offered by the newly developed techniques to assemble (and produce with significant yield) colloidal *molecules*, particles decorated on their surface by a predefined number of attractive sticky spots, i.e., particles with specifically designed shapes and interaction sites [2–5]. These new particles, thanks to the specificity of the built-in interactions, will be able not only to reproduce molecular systems on the nano and micro scale, but will also show novel collective behaviors. To guide future applications of patchy colloids, to help in designing bottom-up strategies in self-assembly [6–8], and to tackle the issue of interplay between dynamic arrest and crystallization—a hot-topic related, for example, to the possibility of nucleating a colloidal diamond crystal structure for photonic applications [9]—it is crucial to be able to predict the region in the (T-ϕ) plane in which clustering, phase separation, or even gelation is expected.

While design and production of patchy colloids is present-day research, unexpectedly theoretical studies of the physical properties of these systems have a longer history, starting in the eighties in the context of the physics of associated liquids [10–15]. These studies, in the attempt to pin down the essential features of association, modeled molecules as hardcore particles with attractive spots on the surface, a realistic description of the recently created patchy colloidal particles. A thermodynamic perturbation theory (TPT) appropriate for these models was introduced by Wertheim [16] to describe association under the hypothesis that a sticky site on a particle cannot bind simultaneously to two (or more) sites on another particle. Such a condition can be naturally implemented in colloids, due to the relative size of the particle as compared to the range of the sticky interaction. These old studies provide a very valuable starting point for addressing the issue of the phase diagram of this new class of colloids, and, in particular, of the role of the patches number.

In this Letter, we study a system of hard-sphere particles with a small number M of identical short-ranged, square-well attraction sites per particle (sticky spots), distributed on the surface with the same geometry as the recently produced patchy colloidal particles [4]. We identify the number of possible bonds per particle as the key parameter controlling the location of the critical point, as opposed to the fraction of surface covered by attractive patches. We present results of extensive numerical simulations of this model in the grand-canonical ensemble [17] to evaluate the location of the critical point of the system in the (T-ϕ) plane as a function of M. We complement the simulation results with the evaluation of the region of thermodynamic instability according to the Wertheim theory [16,18,19]. Both theory and simulation confirm that, on decreasing the number of sticky sites, the critical point moves toward smaller ϕ and T values. We note that while adding to hard spheres a spherically symmetric attraction creates a liquid-gas critical point which shifts toward larger ϕ on decreasing the range of interaction, the opposite trend is presented here when the number of interacting sites is decreased. Simulation and theory also provide evidence that for binary mixtures of particles with two and three sticky spots (where $\langle M \rangle$, the average M per particle can be varied continuously down to two by changing the relative concentration of the two species) the critical point shifts continuously toward vanishing ϕ. This makes it possible to realize equilibrium liquid states with arbitrary small ϕ (*empty liquids*), a case which can not be realized via spherical potentials.

We focus on a system of hard-sphere particles (of diameter σ, the unit of length) whose surface is decorated by M sites (see Fig. 1), which we collectively label Γ. The interaction $V(\mathbf{1}, \mathbf{2})$ between particles $\mathbf{1}$ and $\mathbf{2}$ is

$$V(\mathbf{1}, \mathbf{2}) = V_{\mathrm{HS}}(\mathbf{r}_{12}) + \sum_{A \epsilon \Gamma} \sum_{B \epsilon \Gamma} V_W^{AB}(\mathbf{r}_{AB}) \qquad (1)$$

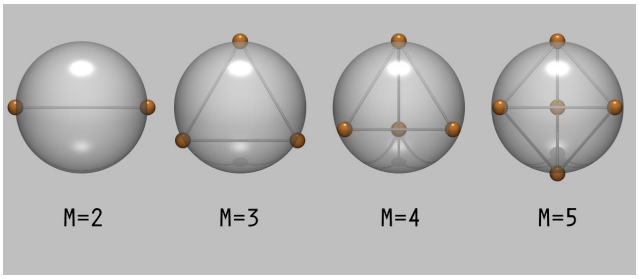

FIG. 1 (color online). Schematic representation of the location of the square-well interaction sites (centers of the small spheres) on the surface of the hardcore particle. Sticks between different interaction sites are drawn only to help visualize the geometry.

where the individual sites are denoted by capital letters, V_{HS} is the hard-sphere potential, $V_W^{AB}(x)$ is a well interaction (of depth $-u_0$ for $x \leq \delta$, 0 otherwise), and $\mathbf{r}_{12}$ and $\mathbf{r}_{AB}$ are, respectively, the vectors joining the particle-particle and the site-site centers [20]. Geometric considerations for a three touching spheres configuration show that the choice $\delta = 0.5(\sqrt{5 - 2\sqrt{3}} - 1) \approx 0.119$ guarantees that each site is engaged at most in one bond. With this choice of δ, M is also the maximum number of bonds per particle. Temperature is measured in units of u_0 (i.e., Boltzmann constant $k_B = 1$).

To locate the critical point, we perform grand-canonical Monte Carlo (GCMC) simulations and histogram reweighting [21] for $M = 5$, 4 and 3 and for binary mixtures of particles with $M = 3$ (fraction α) and $M = 2$ (fraction $1 - \alpha$) at five different compositions, down to $\langle M \rangle \equiv 3\alpha + 2(1 - \alpha) = 2.43$. We implement MC steps composed each by 500 random attempts to rotate and translate a random particle and one attempt to insert or delete a particle. On decreasing $\langle M \rangle$, numerical simulations become particularly time consuming, since the probability of breaking a bond $\sim e^{1/T}$ becomes progressively small. To improve statistics, we average over 15–20 independent MC realizations. Each of the simulations lasts more than 10^6 MC steps. After choosing the box size, the T and the chemical potential μ of the particle(s), the GCMC simulation evolves the system toward the corresponding equilibrium density. If T and μ correspond to the critical point values, the number of particles N and the potential energy E of the simulated system show ample fluctuations. The linear combination $x \sim N + sE$ (where s is named field mixing parameter) plays the role of order parameter of the transition. At the critical point, its fluctuations are found to follow a known universal distribution, i.e. (apart from a scaling factor), the same that characterizes the fluctuation of the magnetization in the Ising model [21]. Recent applications of this method to soft matter can be found in Ref. [22–24].

Figure 2 shows the resulting density fluctuations distribution $P(\phi)$ at the estimated critical temperature T_c and critical chemical potential(s) μ_c for several M values[25]. The distributions, whose average is the critical packing

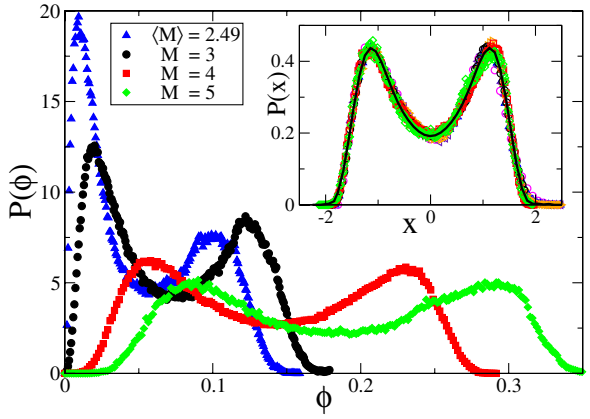

FIG. 2 (color online). Density fluctuations distribution $P(\phi)$ in the GCMC simulations at the critical point for four of the studied M values. The inset shows $P(x)$ for all studied cases, compared with the expected distribution (full line) for a system at the critical point of the Ising universality class [21].

fraction ϕ_c, shift to the left on decreasing M and become more and more asymmetric, signalling the progressive increasing role of the mixing field. In the inset, the calculated fluctuations of x, $P(x)$, are compared with the expected fluctuations for systems in the Ising universality class [21] to provide evidence that (i) the critical point has been properly located; (ii) the transition belongs to the Ising universality class in all studied cases. The resulting critical parameters are reported in Table I. Data show a clear monotonic trend toward decreasing T_c and ϕ_c on decreasing M.

Differently from the ϕ_c-scale, which is essentially controlled by M, T_c, depends on the attractive well width. Experimentally, values of u_0/k_BT comparable to the ones reported in Table I can be realized by modifying the physical properties (size, polarizability, charge, hydrophobicity) of the patches [3–5] or by functionalizing the surface of the particle with specific molecules [26,27].

One interesting observation steaming from these results is that reduction of M makes it possible to shift ϕ_c to values smaller than $\phi = 0.13$, which is the lowest ϕ_c

TABLE I. Values of the relevant parameters at the critical point. In the one-component case ($M = 3, 4, 5$), μ_c^1 is the critical chemical potential (in units of u_0). In the case of the mixture, μ_c^1 (μ_c^2) is the critical chemical potential of $M = 3$ ($M = 2$) particles. L indicates the largest box size studied.

$\langle M \rangle$	T_c	ϕ_c	μ_c^1	μ_c^2	s	L
2.43	0.076	0.036	−0.682	−0.492	0.70	9
2.49	0.079	0.045	−0.646	−0.483	0.64	9
2.56	0.082	0.052	−0.611	−0.478	0.57	9
2.64	0.084	0.055	−0.583	−0.482	0.57	9
2.72	0.087	0.059	−0.552	−0.493	0.52	9
3	0.094	0.070	−0.471	⋯	0.46	9
4	0.118	0.140	−0.418	⋯	0.08	7
5	0.132	0.185	−0.410	⋯	0	7

possible for attractive spherical potentials. Indeed, for spherical square-well potentials $0.13 < \phi_c < 0.27$, the two limits being provided by the van der Waals model (in which repulsion is modeled by the Carnahan-Starling expression) and by recent numerical analysis of the Baxter model[22], respectively, with infinite and infinitesimal interaction range. We also note that results are consistent with those based on a toy model where an *ad hoc* constraint was added to limit valency [28] and also with previous studies of particles interacting with nonspherical potentials [29,30].

Visual inspection of the configurations for small $\langle M \rangle$ shows that the system is composed by chains of two-coordinated particles providing a link between the three-coordinated particles, effectively renormalizing the bonding distance between the $M = 3$ particles. On adding more $M = 2$ particles, the bonding distance between $M = 3$ particles increases, generating smaller and smaller ϕ_c.

To extend the numerical results beyond the point where it is currently possible to properly perform GCMC simulations (at the lowest $\langle M \rangle$, each calculation of the 20 studied samples requires about 1 month of CPU time on a 3.1 GHz processor) and to complement the numerical results, we solve the first-order Wertheim TPT [16,18,19] for the same model (Eq. (1)). The theory can be applied both to one-component systems ($M = 3$, 4, 5) and to binary mixtures ($\langle M \rangle$ spans continuously the region from $M = 2$—where no critical point is present—to $M = 3$) [31].

In TPT, the free energy of the system is written as the Helmholtz HS reference free energy $A_{\rm HS}$ plus a bond contribution $A_{\rm bond}$, which derives by a summation over certain classes of relevant graphs in the Mayer expansion [19]. The fundamental assumption is that the conditions of steric incompatibilities are satisfied: (i) no sites can be engaged in more than one bond; (ii) no pair of molecules can be double bonded. The chosen δ guarantees that the steric incompatibilities are satisfied in the present model. In the more transparent (but equivalent) formulation of Ref. [32], $A_{\rm bond}$ is written as

$$\frac{\beta A_{\rm bond}}{N} = \sum_{A \epsilon \Gamma} \left(\ln X_A - \frac{X_A}{2} \right) + \frac{1}{2} M. \qquad (2)$$

Here X_A is the fraction of sites A that are not bonded. The X_As are obtained from the mass-action equation

$$X_A = \frac{1}{1 + \sum_{B \epsilon \Gamma} \rho X_B \Delta_{AB}} \qquad (3)$$

where $\rho = N/V$ is the total number density and Δ_{AB} is defined by

$$\Delta_{AB} = 4\pi \int g_{\rm HS}(r_{12}) \langle f_{AB}(12) \rangle_{\omega_1, \omega_2} r_{12}^2 dr_{12}. \qquad (4)$$

Here $g_{\rm HS}(12)$ is the reference HS fluid pair correlation function, the Mayer f-function is $f_{AB}(12) = \exp(-V_W^{AB}(\mathbf{r}_{AB})/k_B T) - 1$, and $\langle f_{AB}(r_{12}) \rangle_{\omega_1, \omega_2}$ [33] represents an angular average over all orientations of molecules 1 and 2 at fixed relative distance r_{12}.

The evaluation of Δ_{AB} requires an expression for $g_{\rm HS}(r_{12})$ in the range where bonding occurs. We have used the linear approximation [12]

$$g_{\rm HS}(r) = \frac{1 - 0.5\phi}{(1 - \phi)^3} - \frac{9}{2} \frac{\phi(1 + \phi)}{(1 - \phi)^3} (r - 1) \qquad (5)$$

which provides the correct Carnahan-Starling [34] value at contact.

To locate the critical point, we calculate the equation of state $P(V, T) \equiv -\partial(A_{\rm HS} + A_{\rm bond})/\partial V_T$ and search for the T and ϕ value at which both the first and the second volume (V) derivative of the pressure (P) along isotherms vanish. Figure 3 shows a quantitative comparison of the numerical and theoretical estimates for the critical parameters T_c and ϕ_c. Theory predicts quite accurately T_c but slightly underestimates ϕ_c, nevertheless clearly confirms the M dependence of the two quantities. The overall agreement between Wertheim theory and simulations reinforces our confidence in the theoretical predictions and supports the possibility that on further decreasing $\langle M \rangle$, a critical point at vanishing ϕ can be generated.

TPT allows us also to evaluate the locus of points where $\partial P/\partial V_T = 0$, which provide (at mean field level) the spinodal locus. The predicted spinodal lines in the (T-ϕ) plane for several M values are shown in Fig. 4. On decreasing M also the liquid spinodal boundary moves to lower ϕ values, suggesting that the region of stability of the liquid phase is progressively enhanced. It will be desirable to investigate the structural and dynamical properties of such empty liquids by experimental and numerical work on patchy colloidal particles.

We note that our predictions are relevant to a larger class of functionalized particles, when particle-particle interaction is selective and limited in number. Very new materials

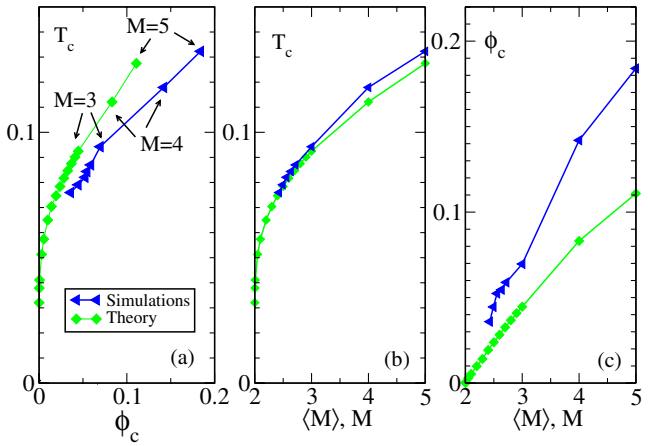

FIG. 3 (color online). Comparison between theoretical and numerical results for patchy particles with different number of sticky spots. Panel (a) shows the location of the points in the (T-ϕ) plane. Panels (b) and (c) compare, respectively, the M dependence for T_c and ϕ_c.

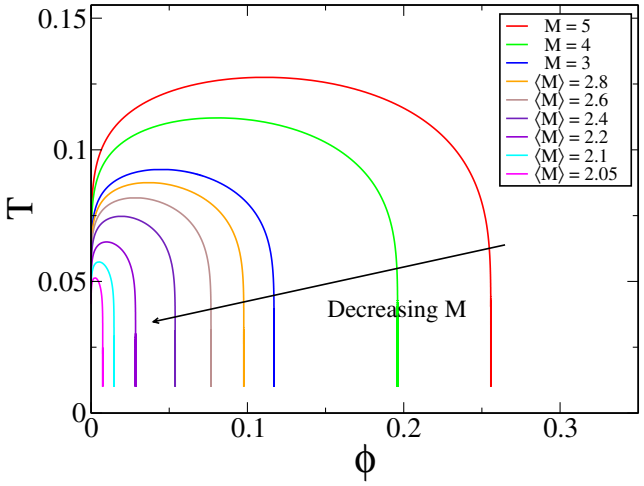

FIG. 4 (color online). Spinodal curves calculated according to TPT for the studied patchy particles for several M and $\langle M \rangle$ values.

belonging to this class are the recently synthesized DNA-coated particles [26]. In this case, M can be varied by controlling the number of strands and the attractive strength can be reversibly tuned by varying the length of the strands. Ratios of u_0/k_BT comparable to the ones discussed here can be realized. Again, the phase diagram of these new materials has not been experimentally measured yet and we hope our work will provide a guideline.

For particles interacting with attractive spherical potentials, phase separation always destabilizes the formation of a homogeneous arrested system at low T. Instead, it is foreseeable that, with small $\langle M \rangle$ patchy particles, disordered states in which particles are interconnected in a persistent gel network can be reached at low T without encountering phase separation. Indeed, at such low T, the bond-lifetime will become comparable to the experimental observation time. Under these conditions, a dynamic arrest phenomenon at small ϕ will take place. It will be thus possible to approach dynamic arrest continuously from equilibrium and to generate a state of matter as close as possible to an ideal gel [35].

The study of the structural and dynamic properties of these low $\langle M \rangle$ equilibrium systems will hopefully help in developing a unified picture of other interesting network formation phenomena taking place at low ϕ [36–40].

We acknowledge support from MIUR-Firb, MIUR-Prin and MCRTN-CT-2003-504712. We thank K. Binder, D. Frenkel and J. Horbach for helpful discussions.

[1] A. Yethiraj and A. van Blaaderen, Nature (London) **421**, 513 (2003).
[2] V. N. Manoharan, M. T. Elsesser, and D. J. Pine, Science **301**, 483 (2003).
[3] Y.-S. Cho *et al.*, J. Am. Chem. Soc. **127**, 15 968 (2005).
[4] D. Zerrouki *et al.*, Langmuir **22**, 57 (2006).
[5] G. Zhang, D. Y. Wang, and H. Möhwald, Angew. Chem., Int. Ed. Engl. **44**, 7767 (2005).
[6] G. M. Whitesides and M. Boncheva, Proc. Natl. Acad. Sci. U.S.A. **99**, 4769 (2002).
[7] S. C. Glotzer, Science **306**, 419 (2004).
[8] S. C. Glotzer, M. J. Solomon, and N. A.Kotov, AIChE J. **50**, 2978 (2004).
[9] M. Maldovan and E. L. Thomas, Nat. Mater. **3**, 593 (2004).
[10] J. Kolafa and I. Nezbeda, Mol. Phys. **61**, 161 (1987).
[11] I. Nezbeda, J. Kolafa, and Y. V. Kalyuzhnyi, Mol. Phys. **68**, 143 (1989).
[12] I. Nezbeda and G. Iglesia-Silva, Mol. Phys. **69**, 767 (1990).
[13] R. P. Sear and J. G. Jackson, J. Chem. Phys. **105**, 1113 (1996).
[14] C. Vega and P. A. Monson, J. Chem. Phys. **109**, 9938 (1998).
[15] M. H. Ford, S. M. Auerbach, and P. A. Monson, J. Chem. Phys. **121**, 8415 (2004).
[16] M. Wertheim, J. Stat. Phys. **35**, 19 (1984).
[17] B. Smit and D. Frenkel, *Understanding Molecular Simulations* (Academic, New York, 1996).
[18] M. Wertheim, J. Stat. Phys. **35**, 35 (1984).
[19] J. P. Hansen and I. R. McDonald, *Theory of Simple Liquids* (Academic Press, New York, 2006), 3rd ed..
[20] The well interaction, among all short-ranged potentials, provides a sharp definition of bonding, avoids multiple bonding (choosing the appropriate δ), and allows for a close comparison with the Wertheim theory.
[21] N. B. Wilding, J. Phys. Condens. Matter **9**, 585 (1997).
[22] M. A. Miller and D. Frenkel, Phys. Rev. Lett. **90**, 135702 (2003).
[23] J. B. Caballero *et al.*, J. Chem. Phys. **121**, 2428 (2004).
[24] R. L. C. Vink and J. Horbach, J. Chem. Phys. **121**, 3253 (2004).
[25] Close to the critical point, the correlation length of the fluctuations becomes larger than the box size, preventing self-averaging of ϕ, resulting in a two-peak distribution.
[26] C. A. Mirkin *et al.*, Nature (London) **382**, 607 (1996).
[27] A. J. Hiddessen *et al.*, Langmuir **16**, 9744 (2000).
[28] E. Zaccarelli *et al.*, Phys. Rev. Lett. **94**, 218301 (2005).
[29] R. P. Sear, J. Chem. Phys. **111**, 4800 (1999).
[30] N. Kern and D. Frenkel, J. Chem. Phys. **118**, 9882 (2003).
[31] G. Chapman, G. Jackson, and K. E. Gubbins, Mol. Phys. **65**, 1057 (1988).
[32] G. Jackson, W. G. Chapman, and K. E. Gubbins, Mol. Phys. **65**, 1 (1988).
[33] M. Wertheim, J. Chem. Phys. **85**, 2929 (1986).
[34] N. F. Carnahan and K. E. Starling, J. Chem. Phys. **51**, 635 (1969).
[35] F. Sciortino *et al.*, Comput. Phys. Commun. **169**, 166 (2005).
[36] P. I. C. Teixeira, J. M. Tavares, and M. M. Telo da Gama, J. Phys. Condens. Matter **12**, R411 (2000).
[37] T. Tlusty and S. A. Safran, Science **290**, 1328 (2000).
[38] E. Del Gado and W. Kob, Europhys. Lett. **72**, 1032 (2005).
[39] F. Sciortino and P. Tartaglia, Adv. Phys. **54**, 471 (2005).
[40] J. T. Kindt, J. Phys. Chem. B **106**, 8223 (2002).